JOURNAL OF AIRCRAFT
Vol. 32, No. 4, July–August 1995

Flow Developments Above 50-Deg Sweep Delta Wings with Different Leading-Edge Profiles

J. J. Miau,* K. T. Kuo,† W. H. Liu,† S. J. Hsieh,‡ and J. H. Chou§
National Cheng Kung University, Tainan 70101, Taiwan, Republic of China
and
C. K. Lin¶
Chung Shan Institute of Science and Technology, Taichung, Taiwan, Republic of China

The characteristics of flow developments above 50-deg sweep delta wings with different leading-edge profiles are shown by flow visualizations and velocity measurements. The Reynolds number based on freestream velocity and root chord is about 7×10^3. The leading-edge profiles studied include the shapes of square, round, windward surface beveling, leeward surface beveling, and wedge. Based on the velocity data obtained along the leading edges of the delta wings it is noted that the flow angles associated with the separated shear layers vary with the leading-edge profiles studied. This finding infers that varying the leading-edge profile has an impact on the initial development of the separated shear layer, consequently, the formation of leading-edge vortex. Furthermore, it is shown that the leading edge of windward beveling causes the largest leading-edge flow angle and produces the most organized leading-edge vortex.

Introduction

DELTA wing models employed for experimental studies are frequently characterized by sharp leading-edge profiles. Accumulation of experimental evidence shows that the characteristics of the leading-edge vortex flow above a sharp leading-edge delta wing persist over a wide range of Reynolds numbers. This phenomenon can be perceived from the fact that a delta wing at an angle of attack forces the windward flow to separate at the leading edge, therefore, the location of flow separation that causes vortex formation is insensitive to the Reynolds number. Further, there seems a consensus among the experimentalists that as long as the leading-edge profiles are sharp, the leading-edge profile is not of critical concern. This can be sensed from a review over the previous reports that no statement regarding a standard configuration of the leading-edge profile has been proposed. Table 1 presents a collection of the delta wing models described.[1–26] While most of the delta wing models reported adopt a configuration of the leading-edge beveling on the windward surface, the beveling angles, and thickness ratios, i.e., the thickness of the wing model vs the root chord length, are not unified. Among the references shown in Table 1, few reports except Kegelman and Roos[21] studied the impacts of the leading-edge profile and the thickness ratio on the vortex flow development above the delta wings. Kegelman and Roos[21] performed flow visualization and force measurements of the 70-deg sweep delta wings with nine leading-edge profiles. They found that different leading-edge profiles significantly affect the vortex breakdown location.

This study is concerned with flow developments above delta wing models of the same thickness, but with different leading-edge profiles. The experimental results obtained show that the leading-edge profiles have significant influence on the developments of vortex flow.

Experimental Methods

Experiments were performed in a closed-return water channel. The maximum speed attained in the test section, 60 × 60 cm in cross section, is 40 cm/s. In the present study, the freestream velocity in the test section denoted as U_0 was chosen to be 5 cm/s, at which both the flow visualization and the velocity measurements above the delta wing were performed. A survey over the flowfield in the test section using a hot-film probe indicated that the nonuniformity of the velocity distribution in the test section away from the boundary layers of the test section walls, in terms of the difference between the maximum and minimum velocities measured, was less than 2% and the turbulence intensity measured was below 0.9%.

All of the delta wing models employed have the root chord lengths of 12 cm, and identical sweep angles, 50 deg. Based on the root chord length and the freestream velocity chosen, the Reynolds number is about 7×10^3. At $\alpha = 10$ deg, i.e., the angle of attack frequently chosen in the work, the blockage ratio due to the presence of the delta wing model is less than 1%.

The delta wing models employed are characterized by nine leading-edge profiles shown in Fig. 1, namely square, windward beveling at 25 deg, round, leeward beveling at 15, 25, 35, 45, and 60 deg, respectively, and a wedge with 50-deg included angle. The delta wing model in the test section was

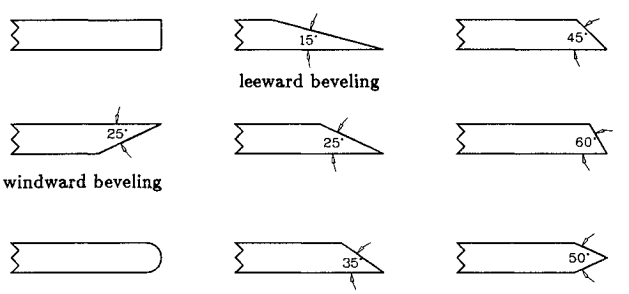

Fig. 1 Leading-edge profiles of the 50-deg sweep delta wings studied.

Received July 28, 1994; revision received Jan. 25, 1995; accepted for publication Jan. 25, 1995.

*Professor, Institute of Aeronautics and Astronautics. Member AIAA.
†Graduate Student, Institute of Aeronautics and Astronautics.
‡Professor, Institute of Aeronautics and Astronautics.
§Professor, Department of Engineering Science.
¶Senior Scientist.

Table 1 Tabulation of typical delta wing configurations in the literature

References	Sweep angle, deg	Leading-edge profile	Thickness ratio, %
1	76	15-deg windward surface beveling	1.6
2	60, 70	25-deg windward surface beveling	2.1, 1.7
3	76	Biconvex surface	3.2
4, 5	52	10-deg windward surface beveling	4.6, 6.2, 4.6
6	80	15-deg windward surface beveling	0.8
7	45–85	15-deg windward surface beveling	0.1 in flat plate
8, 9	70, 75, 80, 85	25-deg windward surface beveling	1.4
10, 11	45, 60	NACA 0012 profile, sharp leading edge	
12	60	Wedge shape	1.8
13	70	23-deg beveling on both surfaces	3.05
14	70	23-deg beveling on both surfaces	3.03
15	70	Wedge shape	2.4
16	63.4, 70, 76	30-deg windward surface beveling	2.08
17	52.5, 60, 67.5, 75	10-deg windward surface beveling	Thin delta wing
18	75	40-deg windward surface beveling	Thin delta wing
19	75	Round	4.2
20	75	24-deg windward surface beveling	1.57
21	70	Nine leading-edge shapes	1.67
22	59, 63.4, 67, 70	Square shape	0.67, 0.67, 0.53, 0.5
23, 24	70	45-deg windward surface beveling	6.25 for half-model, 1.6, 3.1, 6.3 for full-span model
25	55	10-deg windward surface beveling	1.3
26	70	45-deg windward surface beveling	6.3

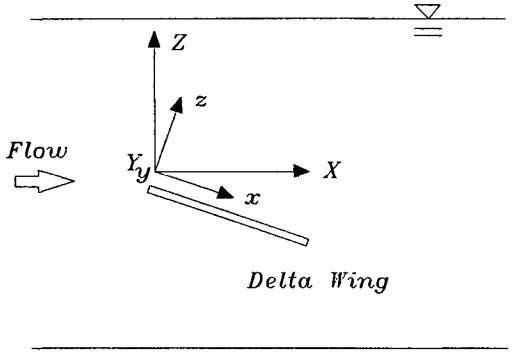

Fig. 2 Two coordinate systems employed in this study.

supported by a sting extended from the rear, which was a circular cylinder 3 mm in diameter. The delta wing models were made of aluminum plates, 5 mm in thickness, corresponding to 4% of the root chord length.

Two techniques of flow visualization were employed for the present work. One was to introduce the color dye from the apex of the delta wing for the purpose of revealing the core of the leading-edge vortex. The dye was introduced by either a stainless-steel tube, 1 mm in diameter, attached beneath the wing model, or the tube placed upstream of the wing model. The other technique was to apply paint in dots on the leeward surface of the delta wing.[27] Having the delta wing model placed in the test section for a certain length of time, the dots become traces due to the viscous drag of flow near the wing surface. The traces are noted equivalent to the limiting streamlines on a solid surface.[28]

Velocity measurements of the flowfield were made with a two-component laser velocimeter. The velocity data obtained were reduced to the mean velocity components in the X and Y directions shown in Fig. 2, denoted as U and V, respectively. It should be mentioned that in this article two coordinate systems are employed for the convenience of later descriptions. As seen in Fig. 2, X, Y, and Z denote the axes of the laboratory coordinate system, and x, y, and z denote the axes of the coordinate system adhered to the delta wing. The mean velocity component in the Z direction is denoted as W in this work.

Experimental Results

Flow Visualization

Delta Wing with Square Leading-Edge Profile

The results of flow visualization obtained for the delta wing with square leading-edge profile, at $\alpha = 10$ deg, are shown in Fig. 3, which serve as a basis for later comparison. The dye streaks shown in the photograph in Fig. 3a indicate the cores of the leading-edge vortices. As a counterpart of Fig. 3a, the limiting streamline pattern shown in Fig. 3b reveals that two separation lines are formed symmetrically with respect to the root chord, where the separation line is seen as the result of convergence of the traces. The separation lines are referred as a result of the secondary separation on the delta wing, induced by the leading-edge vortices of which the vortex cores are shown in Fig. 3a. Also noted in Fig. 3b is that in the region near the trailing edge of the delta wing, outboard of each of the separation lines, the reversed flow is seen.

It should be mentioned that for the delta wing at $\alpha = 20$ deg and above, the dye streaks released from the apex diffuse immediately downstream, implying no formation of leading-edge vortices above the delta wing. As an example, Fig. 3c presents the limiting streamline pattern obtained at $\alpha = 25$ deg, in which no separation lines such as seen in Fig. 3b are found. Instead, the surface pattern is characterized by reverse flow occurring in the outboard region of the delta wing, particularly near the trailing edge, while forward flow takes place in the neighborhood of the root chord.

Delta Wings with Leading Edges Beveling on the Windward Surface

Figure 4 presents the flow visualization photographs of the delta wing with the leading-edge 25-deg beveling on the windward surface, at $\alpha = 10$ deg. In Fig. 4a, the dye streaks clearly show the formation of vortex cores above the delta wing. Moreover, Fig. 4b indicates that the separation lines formed on the delta wing surface persist until the trailing edge of the delta wing, compared to the separation lines shown in Fig. 3b that appear to curve into a spiral structure near the trailing edge. Hence, this comparison of Figs. 3b and 4b suggests that in the latter case the secondary separation induced by the leading-edge vortex is much more well-organized.

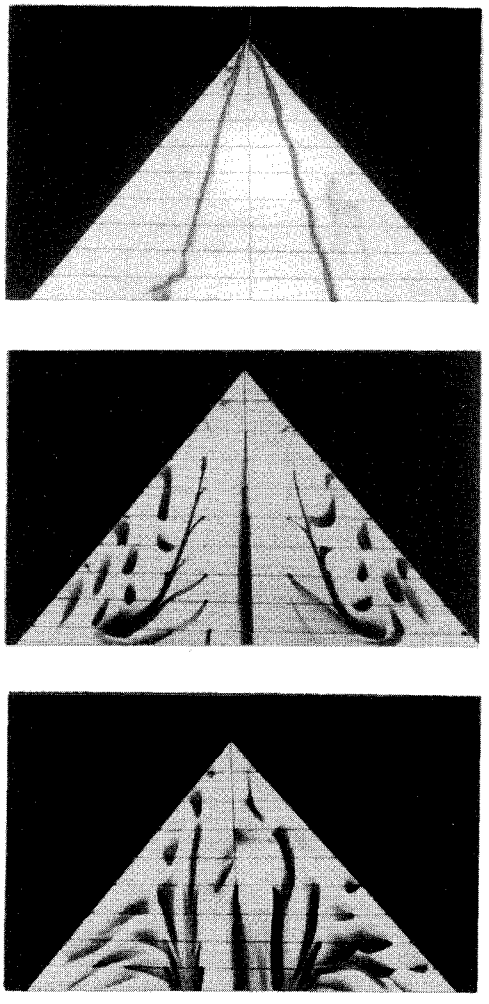

Fig. 3 Flow visualization photographs of the 50-deg sweep delta wing with square leading-edge profile: a) α = 10-deg, dye-streak visualization; b) α = 10-deg, limiting streamline pattern; and c) α = 25-deg, limiting streamline pattern.

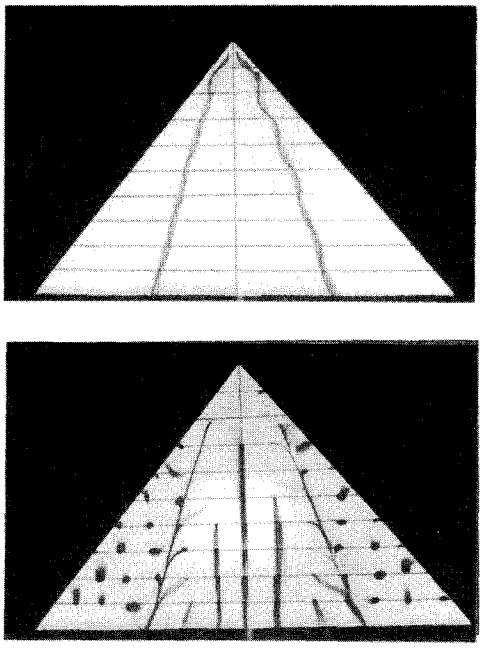

Fig. 4 Flow visualization photographs of the 50-deg sweep delta wing with the leading-edge 25-deg beveling on the windward surface: a) α = 10-deg, dye-streak visualization and b) α = 10-deg, limiting streamline pattern.

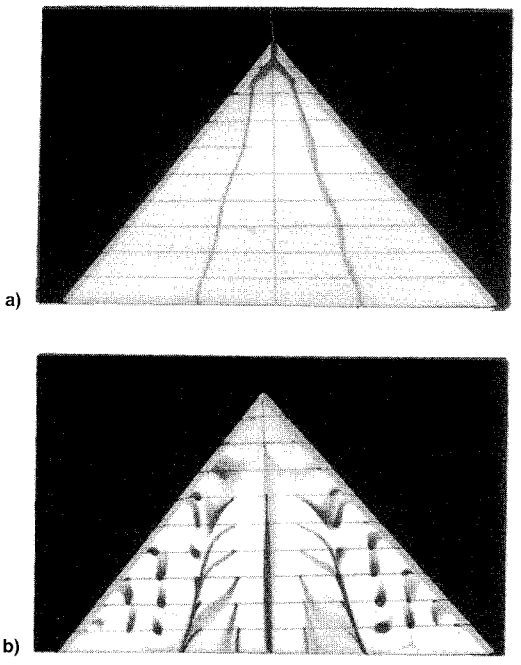

Fig. 5 Flow visualization photographs of the 50-deg sweep delta wing with the leading-edge 60-deg beveling on the leeward surface: a) α = 10-deg, dye-streak visualization and b) α = 10-deg, limiting streamline pattern.

Delta Wings with the Leading-Edges Beveling on the Leeward Surface

Figure 5 presents the flow visualization results of the delta wing with the leading-edge 60-deg beveling on the leeward side, at α = 10 deg, which indicate that the flow characteristics bear similarity to those of the square leading edge and the leading-edge beveling on the windward surface. However, for the cases of the leading-edge beveling angles lower than 60 deg, the flow developments above delta wings are noted to be very different from the foregoing description. These differences are highlightened by the flow visualization results shown in Figs. 6–8, which correspond to the cases of the leading-edge profiles 15-, 25-, and 35-deg beveling on the leeward surface, respectively. Interesting features noted are summarized as follows.

1) At α = 10 deg, the formation of the leading-edge vortex structure is inhibited from these delta wing models. The dye-streak visualization photographs in Figs. 6a, 7a, and 8a do not indicate the formation of vortex core. Furthermore, the limiting streamline patterns in Figs. 7b and 8b show that the separation lines are formed along the interception of the beveling surface and the flat surface on the leeward side, whereas the limiting streamline pattern in Fig. 6b suggests that flow attachment is likely to occur along the interception. All of Figs. 6b, 7b, and 8b indicate no formation of the separation lines associated with the leading-edge vortex development, which are seen in the previous figures.

2) At α = 15 deg, flows over these three delta wings regain the tendency to form the leading-edge vortex structures. For the delta wings with the leading-edges 15- and 35-deg beveling on the leeward surface, this tendency is seen clearly from the dye-streak patterns and the limiting streamline patterns in Figs. 6c and 6d, and Figs. 8c and 8d. The delta wing with the leading-edge 25-deg beveling on the leeward surface corresponds to the least-favorable case toward the formation of the leading-edge vortex structure, shown in Figs. 7c and 7d.

Delta Wing with the Round Leading-Edge Profile

Figure 9 presents the flow visualization results of the delta wing with round leading edge, at α = 10 deg. The photographs

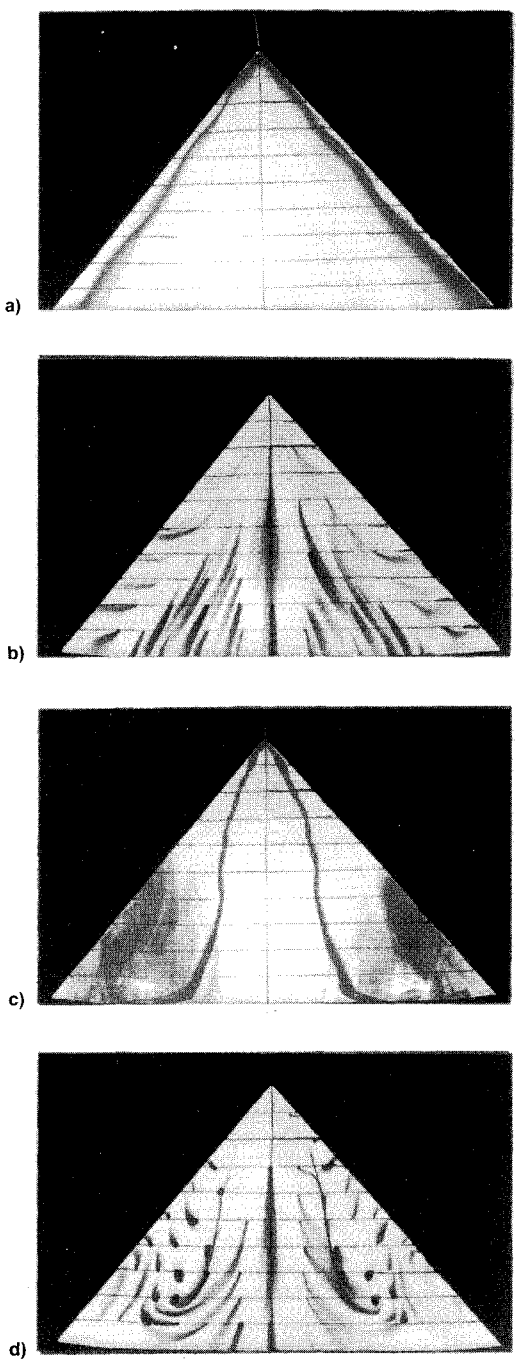

Fig. 6 Flow visualization photographs of the 50-deg sweep delta wing with the leading-edge 15-deg beveling on the leeward surface: a) α = 10-deg, dye-streak visualization; b) α = 10-deg, limiting streamline pattern; c) α = 15-deg, dye-streak visualization; and d) α = 15-deg, limiting streamline pattern.

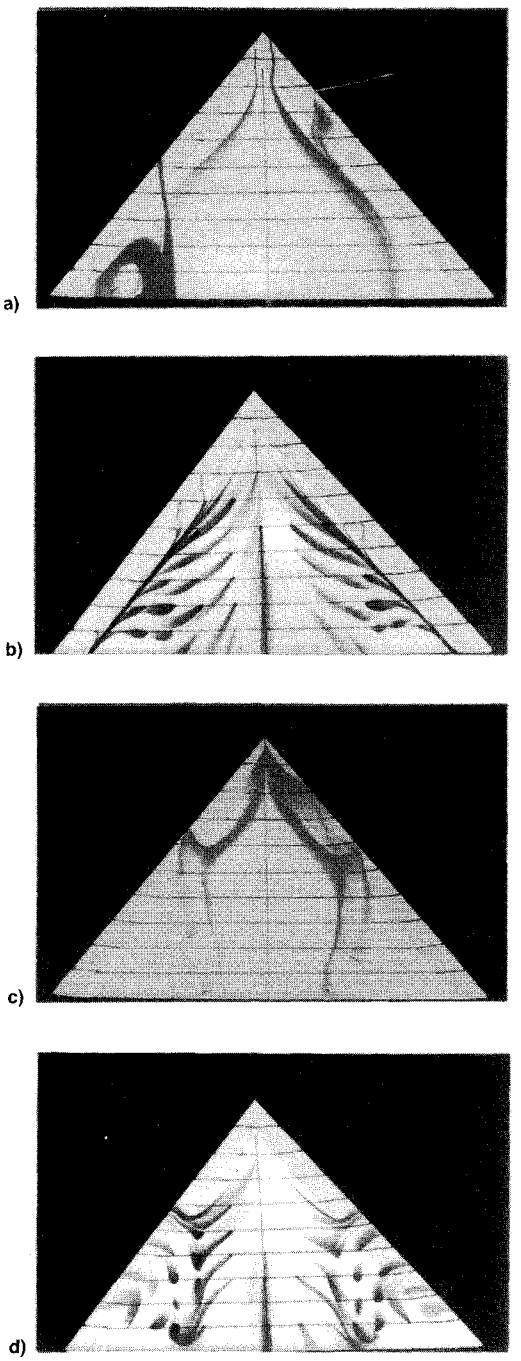

Fig. 7 Flow visualization photographs of the 50-deg sweep delta wing with the leading-edge 25-deg beveling on the leeward surface: a) α = 10-deg, dye-streak visualization; b) α = 10-deg, limiting streamline pattern; c) α = 15-deg, dye-streak visualization; and d) α = 15-deg, limiting streamline pattern.

shown suggest that although the round leading edge is not sharp geometrically, the flow development above the delta wing shows similarity to the cases of square leading-edge profiles, except in the region near the apex. The dye-streak photograph shown in Fig. 9a indicates that the leading-edge vortex develops above the delta wing in the region downstream of $x/C = 0.2$.

Delta Wing with the Leading-Edge in Wedge Shape

Figure 10 presents the flow visualization results of the delta wing with the leading edge in wedge shape, at α = 10 deg. This leading-edge profile is a combination of 25-deg beveling on the windward surface and 25-deg beveling on the leeward surface. The flow visualization photographs shown in this figure suggest no formation of the leading-edge vortex, which falls into the same situation as the delta wing with the leading-edge beveling 25 deg on the leeward surface.

Based on the flow visualization results presented, it can be said that the configuration of the leading-edge beveling on the windward surface can ensure the condition of sharp leading-edge separation, the case most favorable to the formation of the organized vortex structures in this study.

Study of Velocity Field

Laser–Doppler velocity measurements for the selected delta wings at α = 10 deg are presented in this section to describe the quantitative aspects of the differences associated with the variations in the leading-edge profiles.

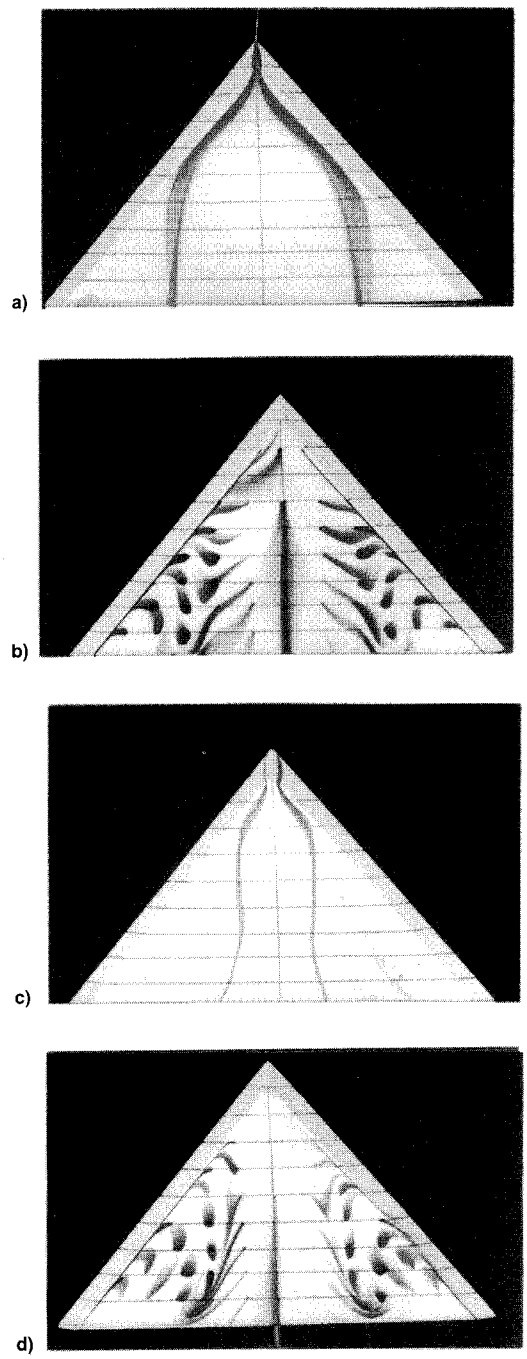

Fig. 8 Flow visualization photographs of the 50-deg sweep delta wing with the leading-edge 35-deg beveling on the leeward surface: a) α = 10-deg, dye-streak visualization; b) α = 10-deg, limiting streamline pattern; c) α = 15-deg, dye-streak visualization; and d) α = 15-deg, limiting streamline pattern.

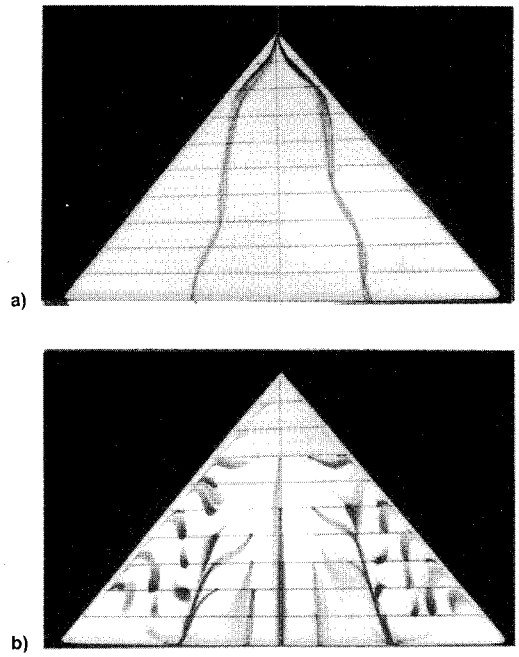

Fig. 9 Flow visualization photographs of the 50-deg sweep delta wing with the leading edge in round shape: a) α = 10-deg, dye-streak visualization and b) α = 10-deg, limiting streamline pattern.

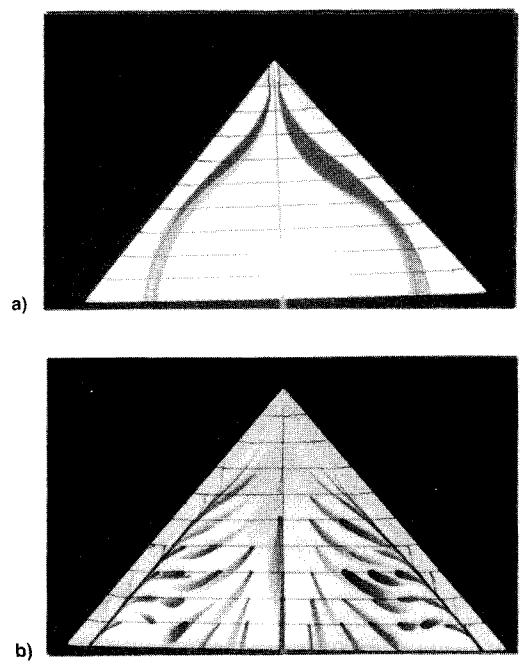

Fig. 10 Flow visualization photographs of the 50-deg sweep delta wing with the leading edge in wedge shape of 50-deg included angle: a) α = 10-deg, dye-streak visualization and b) α = 10-deg, limiting streamline pattern.

Figures 11 and 12 present the streamwise velocity contour plots of the delta wings 25-deg beveling on the windward surface and 25-deg beveling on the leeward surface, respectively, in the Y-Z cross-sectional planes at x/C = 0.3, 0.4, and 0.5. It should be mentioned that for the sake of convenience the measuring volume of the laser velocimeter was traversing with respect to the laboratory coordinates. The velocity measurements were performed over 250–300 grid points for each Y-Z cross-sectional plane intercepting the half-span of the delta wing. In the plots of Figs. 11 and 12, the velocity values shown are normalized by the freestream velocity U_0, and the spatial coordinates are normalized by the length of the local half-span of the delta wing, denoted as S. Here, Y/S = 0 denotes the location of the leading edge and Y/S = 1 denotes the location of the root chord.

A significant difference between Figs. 11 and 12 is noticed. In Fig. 11 the formation of the vortex structure is clearly identified in each of the three cross-sectional planes studied, where the vortex core is referred to as a region of the maximum streamwise velocity measured. On the other hand, in Fig. 12 the characteristics of vortex structure is hardly identifiable, where the region of the maximum streamwise velocity measured is situated very close to the wing surface, which does not allow for a formation of the large-scale vortex struc-

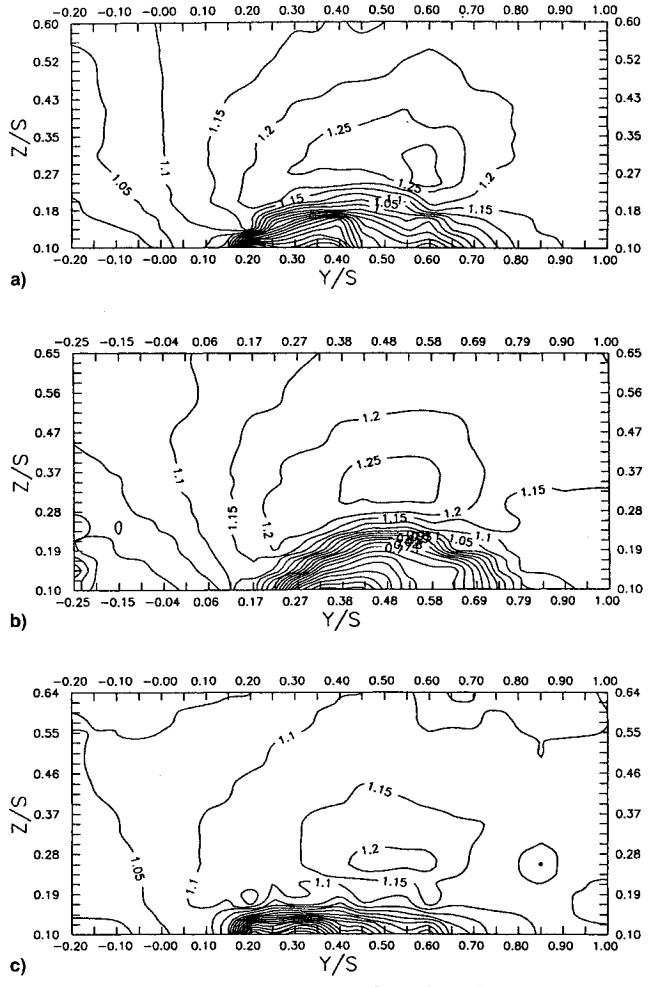

Fig. 11 Streamwise velocity contour plots of the 50-deg sweep delta wing with the leading-edge 25-deg beveling on the windward surface, at α = 10 deg, obtained at x/C = a) 0.3, b) 0.4, and c) 0.5.

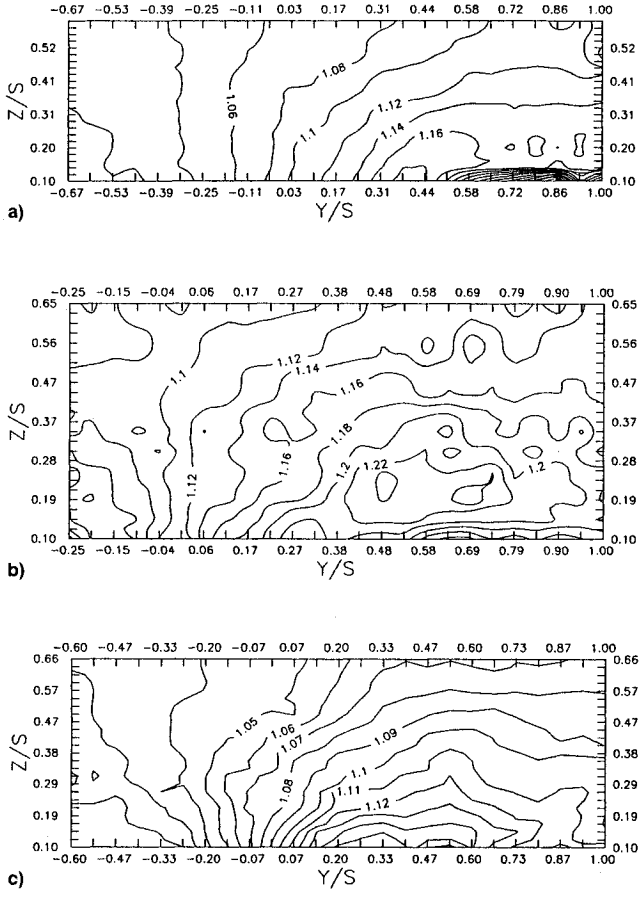

Fig. 12 Streamwise velocity contour plots of the 50-deg sweep delta wing with the leading-edge 25-deg beveling on the leeward surface, at α = 10 deg, obtained at x/C = a) 0.3, b) 0.4, and c) 0.5.

ture. In Fig. 12 the streamwise velocity measured near the wing surface being higher is explained due to the attachment of flow on the leeward surface of the delta wing, rather than the formation of vortex structure. The velocity distributions shown in Fig. 12 are supplement to the flow visualization findings seen in Fig. 7.

In addition to the survey over the velocity fields above the delta wings, velocity measurements were performed along the leading edges of the delta wings to acquire the distributions of flow angle associated with the leading-edge separated shear layer. The measuring volume of the laser velocimeter was positioned 1 mm above the leeward surface of the delta wing at the leading edge. The flow angle mentioned is referred to the angle of a two-dimensional velocity vector measured in the X-Y plane, denoted as $\theta = \tan^{-1}V/U$. At each of the points measured, the flow angle is reduced from five sets of consecutive measurements. Each set of the measurements was performed over a time period of 10 s.

Figure 13 presents the distributions of the flow angle along the leading edges of the delta wings studied. There are two noticeable features in this figure. First, the flow angles associated with the cases of the leading-edges 25-deg beveling on the windward side and on the leeward side appear to be the largest and the smallest, respectively, which can be further correlated with the previous flow visualization results, that in the former case the leading-edge vortex structure appears to be the most well-organized and in the latter case no formation of vortex structure is discerned. Second, for all the cases shown in Fig. 13, the flow-angle distributions are not uniform along the leading edge. Generally speaking, the flow angle

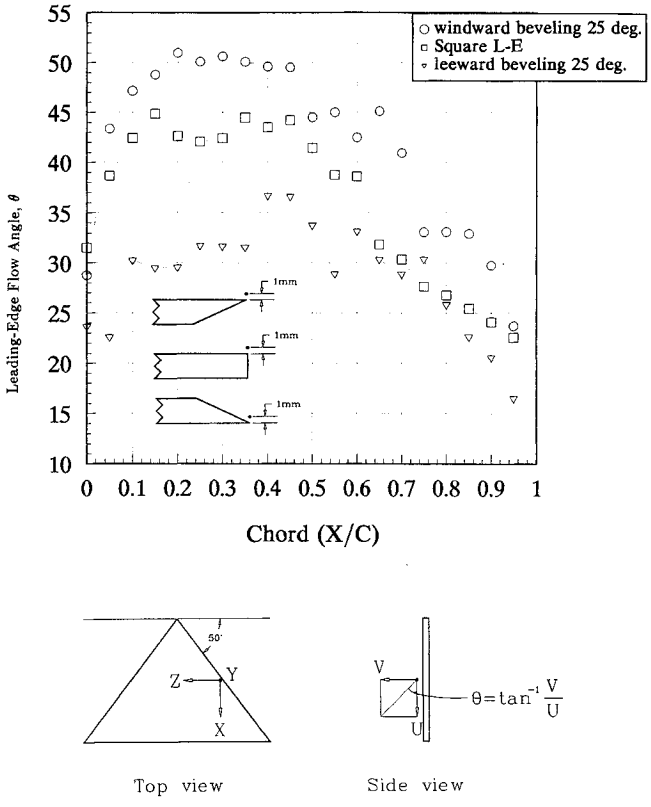

Fig. 13 Flow angle, $\theta = \tan^{-1}V/U$, distributions along the leading edges of the 50-deg sweep delta wings, for α = 10 deg.

increases in the region of $x/C = 0$–0.2, and decreases in the region downstream of $x/C = 0.4$.

Discussion

To understand the flow structures above the delta wings with different leading-edge profiles calls for the need of three-dimensional velocity distributions above the delta wings. Unfortunately, the laser velocimeter employed is limited by its function for two-components velocity measurement only, therefore, the information of the velocity in the third component, i.e., the velocity W in the Z direction, is lacking from direct measurement. Nevertheless, this drawback was overcome by a numerical integration procedure to find W,[27] which is based on the continuity equation for three-dimensional incompressible flow and the U and V velocity data obtained in two neighboring Y-Z cross-sectional planes.

Figure 14 presents the cross-sectional velocity vector plots obtained at $x/C = 0.4$ for two delta wings with the leading-edges 25-deg beveling on the windward surface and on the leeward surface. These velocity vectors are constructed with the mean velocity data of V and W, where the data of W, as mentioned, are deduced from the U and V velocity measurements obtained in the two Y-Z cross-sectional planes at $x/C = 0.39$ and 0.40. In Fig. 14a, the case of the leading-edge beveling on the windward side, the leading-edge vortex is clearly identified in Fig. 14a. The vortex core appears to be at $Z/S = 0.30$ and $Y/S = 0.45$ roughly, which coincides with the location of the maximum streamwise velocity seen in the contour plot of $x/C = 0.4$ in Fig. 11b. Also noted in Fig. 14a is that a region near the wall, at $Y/S = 0.50$–0.15, where the flow convecting strongly along the wing surface toward the leading edge. This is the region of low streamwise velocity measured, shown in Fig. 11b. For the case of the leading-edge beveling on the leeward surface, Fig. 14b shows no indication concerning the formation of the leading-edge vortex. A weak cross-streamwise motion in the region about $Z/S = 0.25$ and $Y/S = 0.30$–0.75 indicates that the flow convects from the leading edge to the root chord, which is seen to promote a weak formation of streamwise vortex in the region of $Z/S < 0.25$. Farther away from the wing surface, the cross-streamwise motion appears in the opposite direction, namely from the root chord to the leading edge.

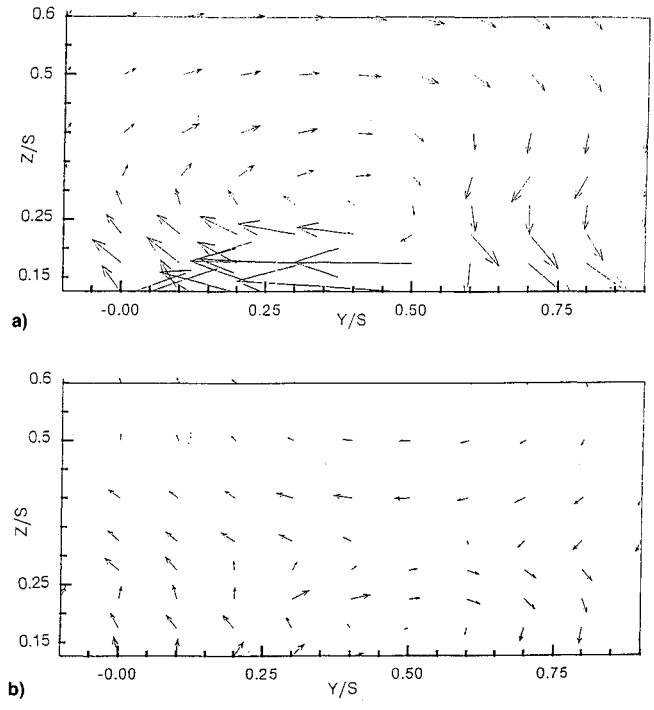

Fig. 14 Cross-sectional velocity vector plots, at $x/C = 0.4$, for the delta wings with the leading-edges 25-deg beveling a) on the windward surface and b) on the leeward surface, at $\alpha = 10$ deg.

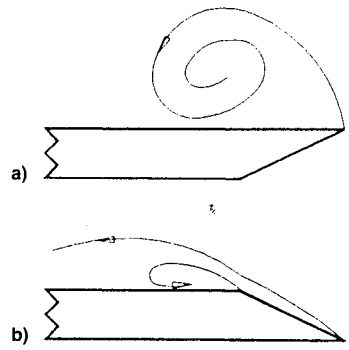

Fig. 15 Sketches of the cross-sectional views of the separated shear layers developed from the leading-edges 25-deg beveling a) on the windward surface and b) on the leeward surface.

Based on the flow visualization results and the velocity measurements presented in the previous figures, two schematic drawings depicting the cross-sectional views of the separated shear layers developed from the leading-edges 25-deg beveling on the windward surface and on the leeward surface are suggested in Figs. 15a and 15b, respectively. The sketch shown in Fig. 15a describes the trajectory of the separated shear layer that reaches farthest away from the delta wing and leads to the formation of organized vortex structure. On the other hand, the sketch shown in Fig. 15b describes the trajectory of the separated shear layer that stays close to the wing surface at the leading edge, and results in a weak formation of vortex structure being developed inboard of the interception of the leeward surface and the beveling surface.

Concluding Remarks

Flow visualizations and velocity measurements obtained for 50-deg sweep delta wings, at $\alpha = 10$ deg mainly, and at the Reynolds number 7×10^3, illustrate that varying the leading-edge profile of the delta wing affects the development of the three-dimensional vortex on the leeward side. The configuration of the leading-edge beveling on the windward surface, which is the most popular in the previous references seen, is found to ensure the formation of the leading-edge vortex structure at $\alpha = 10$ deg. On the other hand, the configuration of the leading-edge beveling on the leeward surface risks to lose the leading-edge vortex above the delta wing at $\alpha = 10$ deg. These notable differences are resorted to that modification in the leading-edge profile affects the initial state of the separated shear layer, as realized from the flow-angle measurements in the X-Y plane along the leading edge, consequently, the trajectory of the separated shear layer above the delta wing. The present results call for the attention to the geometrical shape of the leading-edge profile if a delta wing model is under preparation for experiment.

Acknowledgments

This work was supported by the National Science Council, Republic of China, under Contracts NSC 82-0424-E-006-445 and NSC 82-0618-E-006-481. The first two authors (J. J. M. and K. T. K.) would like to thank R. C. Chang who provided the numerical program for reducing the velocity W in the Z direction.

References

[1]Ayoub, A., and McLachlan, B. G., "Slender Delta Wing at High Angles of Attack—A Flow Visualization Study," AIAA Paper 87-1230, June 1987.

[2]Roos, F. W., and Kegelman, J. T., "An Experimental Investigation of Sweep-Angle Influence on Delta-Wing Flows," AIAA Paper 90-0383, Jan. 1990.

[3]Verhaagen, N. G., and Naarding, S. H. J., "Experimental and Numerical Investigation of the Vortex Flow over a Yawed Delta Wing," AIAA Paper 88-2563, June 1988.

[4]Atta, R., and Rockwell, D., "Leading-Edge Vortices Due to Low Reynolds Number Flow Past a Pitching Delta Wing," *AIAA Journal*, Vol. 28, No. 6, 1990, pp. 995–1004.

[5]Atta, R., and Rockwell, D., "Hysteresis of Vortex Development and Breakdown on an Oscillating Delta Wing," *AIAA Journal*, Vol. 25, No. 11, 1987, pp. 1512, 1513.

[6]Lowson, M. V., "Some Experiments with Vortex Breakdown," *Journal of the Royal Aeronautical Society*, Vol. 68, May 1964, pp. 343–346.

[7]Wentz, W. H., Jr., and Kohlman, D. L., "Vortex Breakdown on Slender Sharp-Edged Wings," *Journal of Aircraft*, Vol. 8, No. 3, 1971, pp. 156–161.

[8]Payne, F. M., Ng, T. T., and Nelson, R. C., "Experimental Study of the Velocity Field on a Delta Wing," AIAA Paper 87-1231, June 1987.

[9]Payne, F. M., Ng, T. T., Nelson, R. C., and Schiff, L. B., "Visualization and Wake Surveys of Vortical Flow over a Delta Wing," *AIAA Journal*, Vol. 26, No. 2, 1988, pp. 137–143.

[10]Gad-el-Hak, M., and Ho, C.-M., "The Pitching Delta Wing," *AIAA Journal*, Vol. 23, No. 11, 1985, pp. 1660–1665.

[11]Gad-el-Hak, M., and Ho, C.-M., "Unsteady Vortical Flow Around Three-Dimensional Lifting Surfaces," Vol. 24, No. 5, 1986, pp. 713–721.

[12]Er-El, J., "The Visualization of the Flowfield About a Delta Wing with Spanwise Blowing," *Experiments in Fluids*, Vol. 6, No. 6, 1988, pp. 419–421.

[13]Thompson, S., Batill, S. M., and Nelson, R. C., "The Separated Flow Field on a Slender Delta Wing Undergoing Transient Pitching Motions," AIAA Paper 89-0194, Jan. 1989.

[14]LeMay, S. P., Batill, S. M., and Nelson, R. C., "Leading Edge Vortex Dynamics on a Pitching Delta Wing," AIAA Paper 88-2559, June 1988.

[15]Soltani, M. R., Bragg, M. B., and Brandon, J. M., "Experimental Measurements on an Oscillating 70-Degree Delta Wing in Subsonic Flow," AIAA Paper 88-2576, June 1988.

[16]Jarrah, M. M., "Low-Speed Wind Tunnel Investigation of Flow About Delta Wings, Oscillating in Pitch to Very High Angle of Attack," AIAA Paper 89-0295, Jan. 1989.

[17]Miller, D. S., and Wood, R. M., "Leeside Flows over Delta Wings at Supersonic Speeds," *Journal of Aircraft*, Vol. 21, No. 9, 1984, pp. 680–686.

[18]Magness, C., Robinson, O., and Rockwell, D., "Instantaneous Topology of the Unsteady Leading-Edge Vortex at High Angle of Attack," *AIAA Journal*, Vol. 31, No. 8, 1993, pp. 1384–1391.

[19]Gu, W., Robinson, O., and Rockwell, D., "Control of Vortices on a Delta Wing by Leading-Edge Vortex of a Delta Wing," *AIAA Journal*, Vol. 31, No. 7, 1993, pp. 1177–1186.

[20]Visser, K. D., and Nelson, R. C., "Measurements of Circulation and Vorticity in the Leading-Edge Vortex of a Delta Wing," *AIAA Journal*, Vol. 31, No. 1, 1993, pp. 104–111.

[21]Kegelman, J., and Roos, F., "Effects of Leading-Edge Shape and Vortex Burst on the Flowfield of a 70 Degree Sweep Delta-Wing," AIAA Paper 89-0086, Jan. 1989.

[22]Miau, J. J., Chang, R. C., Chou, J. H., and Lin, C. K., "Non-uniform Motion of Leading-Edge Vortex Breakdown on Ramp Pitching Delta Wing," *AIAA Journal*, Vol. 30, No. 7, 1992, pp. 1691–1702.

[23]Visser, K. D., Nelson, R. C., and Ng, T. T., "A Flow Visualization and Aerodynamic Force Data Evaluation of Spanwise Blow on Full and Half Span Delta Wings," AIAA Paper 89-0192, Jan. 1989.

[24]Visser, K. D., Iwanski, K. P., Nelson, R. C., and Ng, T. T., "Control of Leading Edge Vortex Breakdown by Blowing," AIAA Paper 88-0504, Jan. 1988.

[25]Shi, A., Wu, J. M., and Vakili, A. D., "An Investigation of Leading-Edge Vortices on Delta Wings with Jet Blowing," AIAA Paper 87-0330, Jan. 1987.

[26]Iwanski, K., Ng, T., and Nelson, R. C., "An Experimental Investigation of Delta Wing Vortex Flow with and Without External Jet Blowing," AIAA Paper 89-0084, Jan. 1989.

[27]Chang, R. C., "Studies of Vortical Flows Developing on Stationary and Pitching Delta Wings," Ph.D. Dissertation, Inst. of Aeronautics and Astronautics, National Cheng Kung Univ., Taiwan, ROC, 1991.

[28]Peak, D. J., and Tobak, M., "Three-Dimensional Separation and Reattachment," *High Angle-of-Attack Aerodynamics*, AGARD/VKI Lecture Series 121, Paper 1, 1982.